Advanced Journal of Chemistry, Section B 1 (2019) 29–36
http://dx.doi.org/10.33945/SAMI/AJCB.2019.1.6

ADVANCED JOURNAL OF CHEMISTRY, SECTION B

Original Research Article

http://www.ajchem–b.com

Adsorptions of Diatomic Gaseous Molecules (H_2, N_2 and CO) on the Surface of $Li^+@C_{16}B_8P_8$ Fullerene–Like Nanostructure: Computational Studies

Shaghayegh Ariaei[1,✉]

Received: 17 December 2019 / Accepted: 22 December 2019 / Published Online: 22 December 2019

ABSTRACT

Density functional theory (DFT) calculations have been performed to investigate the adsorption of hydrogen (H_2), nitrogen (N_2) and carbon monoxide (CO) diatomic gaseous molecules at the surface of Li^+ contained $C_{16}B_8P_8$ fullerene–like nanostructure ($Li^+@C_{16}B_8P_8$). The evaluated results from the optimized structures indicated that the adsorption processes could be taken placed for the interacting gas and fullerene systems. Moreover, the electronic properties indicated that the electrical conductivities of Nano Clusters systems are changed after the adsorption processes, in which it could be a signal for detection or sensing of the existence of the gas in the environment. These changes lead to declining the HOMO/LUMO gap of the Fullerene–Like Nano Cage to its original value. As a finding of this work, it could be mentioned that the $Li^+@C_{16}B_8P_8$ fullerene–like nano cage could be considered as a suitable adsorbent for the CO, N_2 and H_2 gaseous. It means that the utilized $Li^+@C_{16}B_8P_8$ Fullerene–Like Nano Cage can detect the existence of gas in the environment.

Keywords: Density functional theory · Adsorption · Fullerene · Sensor · Diatomic gas

Introduction

Hydrogen (H_2), the third most abundant element on the earth, shows its potential of covering necessary energy for the mobile industry [1]. However, The cost–effective use of this alternative energy resource is not an easy task [2] where the main difficulty is to find materials which can store H_2 with large gravimetric and volumetric densities. Meanwhile, operating under ambient thermodynamic conditions is another issue that has to be considered carefully [3]. Nitrogen (N_2) is also available and applicable gas which its storage and purification are almost problematic [4]. By the discovery of nanotechnology in recent three decades, nanostructures have been utilized as the storage materials for gases with different applications [5]. Not only do the novel structural features of nanostructures such as high surface/volume ratio have significant implications concerning energy storage [6] but also, practical use of nanostructures to remove unwanted gases from the environment has attracted the attention of most researchers [7]. Carbon monoxide (CO) is an underlying cause of air pollution which has harmful effects on the human body's health. Therefore, introducing optimum methodologies

✉ Corresponding author.
E–mail address: shaghayeghariaei9595@gmail.com (S. Ariaei)

[1] Department of Chemical Engineering, Science and Research Branch, Islamic Azad University, Tehran, Iran

and materials for detection and removal of CO from the atmosphere of industrial cities with high CO outputs is highly demanded [8]. Previous studies have been demonstrated that the nanostructures could be employed to store and also remove gas activities [9–15]. In comparison with pure carbon–based nanostructures, other non–carbon–based fullerene–like and tubular Nano–structures or decorated Nano–carbons could be expected as active materials for specific adsorptions of various gases [16–21]. Existence of boron/phosphorous (BP) ring nanostructures with refractory semiconducting behavior has been earlier investigated and reported [22]. The strong covalent bonds in the most stable zinc blende structural phase make the BP nano ring a promising material for electronic devices working under such difficult conditions as high temperatures or destructive environments [23]. Hence, making a decorated nanostructure with characteristic behaviors was proposed in the implementation of BP nano ring in the fullerene. Moreover, application of lithium ion (Li^+) in the fullerene structures could induce specific characters for the resulted structure [24–25]. In this study, first principle calculations have been performed for fullerene to investigate adsorptions of diatomic H_2, N_2 and CO gas molecules on the surface of the $Li^+@C_{16}B_8P_8$ fullerene like nanostructure (Fig. 1). All of these gaseous molecules have high practical interests in industrial, environmental, and energy aspects. Introducing a proper sensing fullerene–like material for detection and storage of diatomic H_2, N_2 and CO gases with high selectivity and efficiency is the main purpose of this study.

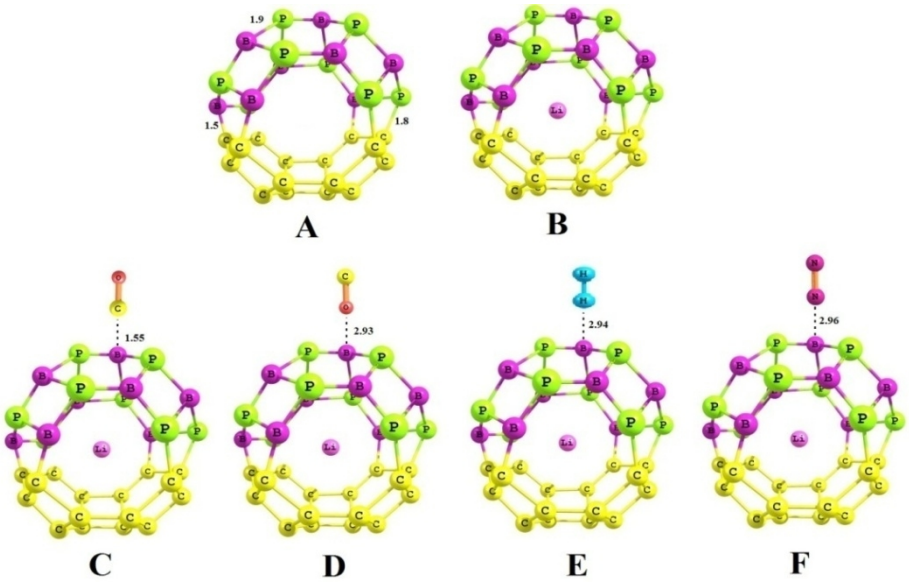

Fig. 1. Optimized geometries of $C_{16}B_8P_8$ and $Li^+@C_{16}B_8P_8$ fullerene–like nanostructures.

Materials and Methods

All calculations of this work are performed by using the M06–2X, DFT method, Due to the dispersion properties and weak interactions by the 6–311G(d,p) [26] level of theory as implemented in a locally modified version of the GAMESS program [27]. The models of study include individual H_2, N_2, CO and $Li^+@C_{16}B_8P_8$ molecules and combinations of each of gases and $Li^+@C_{16}B_8P_8$ fullerene–like nanostructure. Optimized geometries, natural bond orbitals (NBO), molecular electrostatic potentials (MEP), densities of states (DOS), frontier molecular orbitals (FMO) analyses, and energies are evaluated for all models at the mentioned theoretical level (Table 1). The adsorption energy (E_{ad}) is obtained using eq. (1).

$$E_{ads} = E_{(Gas+Fullerene)} - E_{(Gas)} - E_{(Fullerene)} \quad (1)$$

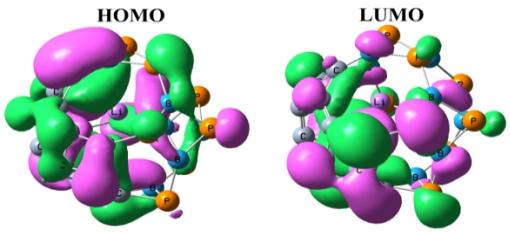

Fig. 2. The HOMO and LUMO 3D shapes of the $Li^+@C_{16}B_8P_8$ fullerene–like nanostructure.

Results and Discussion

The geometries of $C_{16}B_8P_8$ fullerene–like nanostructure were optimized and then the Li^+ ion was added to the center of fullerene to construct $Li^+@C_{16}B_8P_8$ for reoptimization. It should be noted that the structure of $Li^+@C_{16}B_8P_8$ is more stable than the $C_{16}B_8P_8$. The optimized structures for both of $C_{16}B_8P_8$ and $Li^+@C_{16}B_8P_8$ fullerene–like nanostructures are shown in panels A and B of Fig. 1. In contrast to the original carbon fullerene, the fullerene–like nanostructure of this work consists of four different atomic types which are the primary constructing C, B and P atoms and the centralized Li^+ ion in the fullerene. Energy gap (E_g) of the $Li^+@C_{16}B_8P_8$ nanostructures calculated was about 3.62 eV, showing a semiconducting character. As it has indicated in Fig. 2, the highest occupied and the lowest unoccupied molecular orbitals (HOMO and LUMO) of the $Li^+@C_{16}B_8P_8$ are localized on the B, C, and P atoms, respectively, which shows that the B atoms could act as electron deficient centers towards the electron donor molecules.

Table 1: Adsorption energies (E_{ads}), net partial charges (QT) on small gaseous molecules, HOMO–LUMO energy gaps (E_g) of mentioned systems (Fig. 1).

Configuration	E_{ads} (eV)	QT	E_g (eV)	ΔE_g (eV) [a]
A	—	—	3.68	—
B	—	—	3.62	—
C	–0.76	0.429	3.60	0.011
D	–0.11	0.022	3.62	0.001
E	–0.03	0.004	3.61	0.004
F	–0.12	0.032	3.61	0.004

[a] The changes of E_g of nanostructure upon the adsorption process.

3.1. Small molecules adsorption

Diatomic gaseous molecules of H_2, N_2 and CO were chosen as targets to adsorb on the surface of the $Li^+@C_{16}B_8P_8$ fullerene–like nanostructure. Full structural optimizations were carried out for individual and complex structures to examine the energies, equilibrium geometries, and electronic properties. For each of gaseous molecules, numbers of orientations at different atomic sites (C, B, and P) of $Li^+@C_{16}B_8P_8$ nanostructure were considered to explore the best intermolecular geometries of adsorption processes. After doing calculations of full relaxation, the obtained stable configurations, which are corresponding to minimum energies with equilibrium nanostructure gas distances, are defined as the center to center distance of nearest atoms between the nanostructure and the small gaseous molecules (Fig. 1). More details about the values of E_{ads}, NBO charge transfer (QT) [28] and ΔE_g (change of E_g of nanostructure upon the adsorption process) are listed in Table 1. In the next step, we explore the adsorption of small gaseous molecules one by one.

3.2. CO adsorption by the nanostructure

All possible adsorption configurations of the CO gaseous molecule at the surface of $Li^+@C_{16}B_8P_8$ fullerene–like nanostructure were investigated to understand the correct interaction process between the two molecular counterparts. After

full optimizations, two perpendicular configurations of CO to the nanostructure were found as the most stable ones. (1) The C head of CO is close to the B atom of the nanostructure (Configuration A, Fig. 1C). (2)The O head of CO is close to the B atom of the nanostructure (Configuration B, Fig. 1D). According to the information of Table1, for configuration A, E_{ads} and the interaction distance are –0.76 eV and 1.55 Å, respectively, which accompanied with a charge transfer of 0.430 |e| from CO to the nanostructure .For configuration B, Eads and interaction distance are –0.11 eV and 2.93 Å, respectively, were accompanied with the charge transfer of 0.22 |e| from CO to the nanostructure. Comparing information of A and B configurations, indicates that the former configuration is more favorable than the latter one. Indeed, the calculated MEP plot for configuration A (Fig. 3A) demonstrates that the CO molecule acts as an electron donor versus the electron acceptor nanostructure. Rationalizing the interactions indicates that the adsorption of CO by the nanostructure could be considered as chemical and physical adsorptions for configuration A and B, respectively. Hence, the $Li^+@C_{16}B_8P_8$ fullerene–like nanostructure could be supposed as a proper candidate for sensing the diatomic CO gaseous molecule.

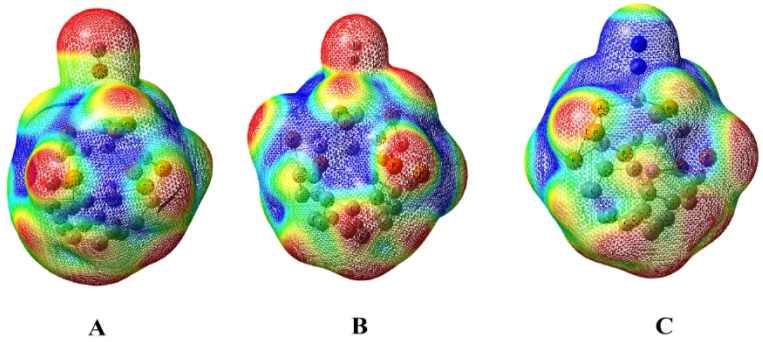

Fig. 3. Calculated molecular electrostatic potential surfaces for (A) CO adsorbed on the $Li^+@C_{16}B_8P_8$ from its C atom and (B) H_2 adsorbed on the $Li^+@C_{16}B_8P_8$ from its H atom, and (C) N_2 adsorbed on the $Li^+@C_{16}B_8P_8$ from its N atom. The surfaces are defined by the 0.0004 electrons/b3 contour of the electron density. Color ranges, in a.u.: blue, more positive than 0.050; red, more negative than –0.050and green neutral.

3.3. H_2 adsorption by the nanostructure

Possible configurations of relaxed H_2 gaseous molecule at the surface of $Li^+@C_{16}B_8P_8$ fullerenes–like nanostructure have been investigated to find the best interacting system of two molecular counterparts. In one of configurations, the H_2 molecule was first placed above the B atom, but it was reoriented into perpendicular to the nanostructure surface. In other configurations, placement of H_2 molecule parallel to the nanostructure surface, above the center of tetragonal and hexagonal rings, were also examined. After calculating full relaxations, the most stable complex was obtained with E_{ads} of –0.03 eV and interaction distance of 2.94 Å (Fig. 1E). In the obtained configuration (Fig. 1E), the adsorbed H_2 axis is parallel to the nanostructure surface and the H atom is close to the B atom accompanied by a charge transfer of 0.004 |e| from the H_2 to the nanostructure (refer to Table 1). The obtained information revealed that H_2 gaseous molecule could be detected by the $Li^+@C_{16}B_8P_8$ fullerene–like nanostructure through physical adsorption.

3.4. N_2 adsorption by the nanostructure

The N_2 gaseous molecule was placed on the surface of $Li^+@C_{16}B_8P_8$ fullerene–like nanostructure in different orientations to find the optimal adsorption conditions. The most favorable

configuration of N_2 on the nanostructure is shown in Fig. 1F. The interactions between B atom of the nanostructure and N atom of N_2 molecule, after calculations full relaxation, yielded – a configuration with the perpendicular alignment of adsorbed N_2 on the nanostructure surface. Within this process, E_{ads}= –0.12 eV and interaction distance= 2.96 Å have been obtained. The interaction between two molecular counterparts caused a charge transfer of –0.032 |e| from N_2 to nanostructure (refer to Table 1). The interaction of N_2 with nanostructure is localized on the B atom with a physical adsorption condition. From all discussions up to now, it could be concluded that the adsorption energy favorability is in order of CO>N_2>H_2, regarding the most stable complexes.

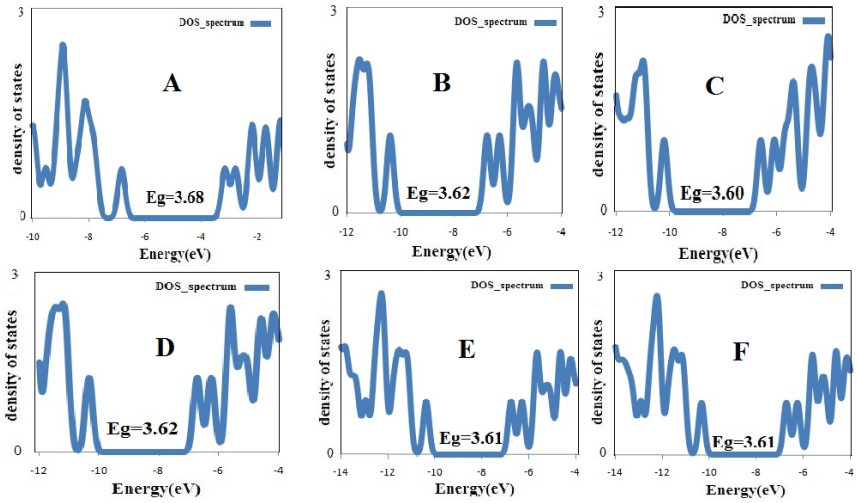

Fig. 4. Calculated density of states for pristine $C_{16}B_8P_8$ cluster (A), Li^+@$C_{16}B_8P_8$ cluster (B), CO@cluster(i) (C) , CO@cluster(ii) (D), H_2@cluster (E), N_2@cluster (F).

3.5. Density of states

To verify effects of the adsorption of small molecules on the cluster electronic properties electronic density of states (DOS) of the cluster and adsorbates/cluster complexes were calculated (Fig. 4). For the configuration B, it can be found that the DOS near the Fermi level are not affected by the CO adsorption (Fig. 4 C). So the *E*g of cluster has change upon the CO adsorptions (ΔE_g = 0.011 for the C). Upon the CO adsorption in the configuration, only intensity of the LUMO virtual state at level is promoted and no impurity state is observed in the electron forbidden region of E_g. Thus, the Li^+@$C_{16}B_8P_8$ nanocluster can be an appropriate sensor for CO in configuration C detection. As depicted the DOSs in Fig. 4, in the other configurations upon the H_2 and N_2 adsorption some energy states appear above the Fermi level so that the Fermi level shifts to lower energy levels. The E_g of the nanocluster has change (ΔE_g = 0.04 and 0.04 eV in the other configurations, respectively (Table1). This occurrence is expected to bring about obvious change in the corresponding electrical conductivity because it is well known that the E_g (or band gap in bulk materials) is a major factor determining the electrical conductivity of a material and a classic relation between them is shown in eq. (2) [29].

$$\sigma \alpha \exp\left(\frac{-E_g}{2kT}\right) \quad (2)$$

where σ is the electrical conductivity and k is the Boltzmann's constant.

According to eq. (2), the smaller E_g at a given temperature leads to the higher electrical conductivity. However, the E_g of CO/cluster complex is reduced compared to that of the

pristine cluster. Since the conductivity is exponentially correlated with a negative value of E_g, it is expected that it becomes larger with reducing the E_g. It demonstrates the high sensitivity of the electronic properties of $Li^+@C_{16}B_8P_8$ towards the adsorption of the CO in configuration C molecule. We believe that the $Li^+@C_{16}B_8P_8$ nano–cage can transform the presence of the CO molecules directly into an electrical signal, therefore, could be potentially used in CO sensor devices. However, the electronic properties of nanocluster are not sensitive to the presence of CO gas in configuration D. Hence, it can be deduced that $Li^+@C_{16}B_8P_8$ nanocage selectively acts as a gas sensor device CO configuration C. It is worth to note that the ability of atomic scale study is an advantage of computational works to reveal insightful information about the systems [30–33].

Conclusion

We performed DFT calculations to study the adsorption of H_2, N_2 and CO gaseous molecules on the surface of the $Li^+@C_{16}B_8P_8$ nanostructure. The adsorption energies of the most stable states are calculated to be –0.76eV for CO molecule. In particular, the Li^+@CBP heterogeneous nanostructure is found to be a good candidate for applying in sensor devices. Based on the density of state analysis, it was found that the CO adsorption could increase the electrical conductivity of the fullerene–like Li^+@CBP and reduce its HOMO/LUMO energy gap. Thus, the $Li^+@C_{16}B_8P_8$ heterogeneous nanostructure could be used as a gas sensor device against the CO molecule.

Acknowledgments

I gratefully thank Dr. Milad Nouraliei for his helpful supports of this work.

References

1. A. Herzog, M. Tatsutani; A hydrogen future?. Natural Resources Defense Council. Issued Paper: November (2005).
2. K.T. Busby; Seeking sustainability: Adopting sustainable and renewable energy sources to create a maintable world. Inquiries J. 4 (2012) 1.
3. J. Zhou, Q. Wang, Q. Sun, P. Jena, X.S. Chen; Electric field enhanced hydrogen storage on polarizable materials substrates. PNAS 107 (2010) 2801–2806.
4. B. Schreiner, H.J. Reinhardt; Use of industrial gases in petrochemistry. Hydrocarbon Proc. 87 (2008) 1-24.
5. S.S. Mao, S. Shen, L. Guo; Nanomaterials for renewable hydrogen production, storage and utilization. Prog. Natural Sci. 22 (2012) 522–534.
6. M.U. Niemann, S. Srinivasan, A.R. Phani, A. Kumar, D.Y. Goswami, E.K. Stefanakos; Nanomaterials for hydrogen storage applications: A review. J. Nanomater. 2008 (2008) 950967.
7. T.H. Tran, V.T. Nguyen; Copper oxide nanomaterials prepared by solution methods, some properties, and Potential applications: A brief review. Int. Scholarly Res. Not. 2014 (2014) 856592.
8. C.L. Quéré, M.R. Raupach, J.G. Canadell, G. Marland et al.; Trends in the sources and sinks of carbon dioxide. Nature Geosci. 2(2009) 831–836.
9. S. Santucci, S. Picozzi, F. Di Gregorio, L. Lozzi, C. Cantalini, L. Valentini, J.M. Kenny, B. Delley; NO and CO gas adsorption on carbon nanotubes: Experiment and theory. J. Chem. Phys. 20 (2003) 10904–10910.
10. T.C. Dinadayalane, J. Leszczynski; Remarkable diversity of carbon–carbon bonds: structures and properties of fullerenes, carbon nanotubes, and grapheme. Struct. Chem. 6 (2010) 1155–1169.

11. J.H. Guo, H. Zhang; The effect of electric field on hydrogen storage for B/C/N sheets. Struct. Chem. 22 (2011) 1039–1045.
12. T.C. Dinadayalane, A. Kaczmarek, J. Lukaszewicz, J. Leszczynski; Chemisorption of hydrogen atoms on the sidewalls of armchair single–walled carbon nanotubes. J. Phys. Chem. C 20 (2007) 7376–7383.
13. A. Kaczmarek, T.C. Dinadayalane, J. Lukaszewicz, J. Leszczynski; Effect of tube length on the chemisorptions of one and two hydrogen atoms on the sidewalls of (3,3) and (4,4) single–walled carbon nanotubes: A theoretical study. Int. J. Quant. Chem. 12 (2007) 2211–2219.
14. T.C. Dinadayalane, J. Leszczynski; Stone–wales defects with two different orientations in (5, 5) single–walled carbon nanotubes: A theoretical study. Chem. Phys. Lett. 434 (2007) 86–91.
15. T.C. Dinadayalene, J.S. Murray, M.C. Concha, P. Politzer, J. Leszczynski; Reactivities of sites on (5,5) single–walled carbon nanotubes with and without a stone–wales defect. J. Chem. Theor. Comput. 6 (2010) 1351–1357.
16. F.Fallahpour, M. Nouraliei, S.S. Gorgani; Theoretical evaluation of a double–functional heterogeneous nano–sensor. Appl. Surf. Sci. 366 (2016) 545–551.
17. P. A. Ghamsari, M. Nouraliei, S.S. Gorgani; DFT simulation towards evaluation the molecular structure and properties of the heterogeneous $C_{16}Mg_8O_8$ nano–cage as selective nano–sensor for H_2 and N_2 gases. J. Mol. Graph. Model. 70 (2016) 163–169.
18. S.S. Gorgani, M. Nouraliei, S.S. Gorgani; Heterogeneous $C_{16}Zn_8O_8$ nanocluster as a selective CO/NO nanosensor: Computational investigation. Int. J. Environ. Sci. Technol. 13 (2016) 1573–1580.
19. D. Golberg, Y. Bando; Octahedral boron nitride fullerenes formed by electron beam irradiation. Appl. Phys. Lett. 73 (1998) 2441–2443.
20. H. Omidvar, S. Goodarzi, A. Seif, A.R. Azadmehr; Influence of anodization parameters on the morphology of TiO_2 nanotube arrays. Superlat. Microstruct. 50 (2011) 26–39.
21. S.K. Jain, P. Srivastava; Structural stability of nitrogen–doped ultrathin single–walled boron nanotubes: an ab initio study. Comp. Mater. Sci. 50 (2011) 3038–3042.
22. D.C. Pestana, P.P. Power; Nature of the boron–phosphorus bond in monomeric phosphinoboranes and related compounds. J. Am. Chem. Soc. 113 (1991) 8426–8437.
23. V. Ferreira, H.W.L. Alves; Boron phosphide as the buffer–layer for the epitaxial III–nitride growth: A theoretical study, J. Cryst. Growth 310 (2008) 3973–3978.
24. H. Kawabata, H. Tachikawa; DFT study on the interaction of the smallest fullerene C_{20} with lithium ions and atoms. J. Carbon Res. 3 (2017) 15.
25. E. Cuestas, P. Serra; Localization of the valence electron of endohedrally confined hydrogen, lithium and sodium in fullerene cages. Int. J. Mod. Phys. B. 30 (2016) 1650055.
26. C.H. Suresh, T.L. Lincy, N. Mohan, R. Rakhi, Aromatization energy and strain energy of buckminsterfullerene from homodesmotic reactions. J. Phys. Chem. A 119 (2015) 6683–6688
27. M.W. Schmidt, K.K. Baldridge, J.A. Boatz, S.E. Elbert, M.S. Gordon, J.H. Jensen, S. Koseki, N. Matsunaga, K. Nguyen, S. Su, T, Windus, M. Dupuis, J. Montgomery; General atomic and molecular electronic structure system. J. Comput. Chem. 14 (1993)1347–1363.
28. A.E. Reed, L.A. Curtiss, F. Weinhold; Intermolecular interactions from a natural bond orbital, donor–acceptor viewpoint. Chem. Rev. 88 (1988) 899–926.

29. S. Li; Semiconductor Physical Electronics, 2nd Ed., Springer, USA, 2006.
30. H. Nazemi, M. Mirzaei, E. Jafari; Antidepressant activity of curcumin by monoamine oxidase–A inhibition. J. Adv. Chem. B 1 (2019) 3–9.
31. A.N. Esfahani, M. Mirzaei, Flavonoid derivatives for monoamine oxidase–A inhibition. Adv. J. Chem. B 1 (2019) 19–22.
32. O.M. Ozkendir, M. Mirzaei; Alkali metal chelation by 3–hydroxy–4–pyridinone. Adv. J. Chem. B 1 (2019) 10–16.
33. A. Kouchaki, O. Gulseren, N. Hadipour, M. Mirzaei; Relaxations of fluorouracil tautomers by decorations of fullerene–like SiCs: DFT studies. Phys. Lett. A 380 (2016) 2160–2166.

How to cite this article: S. Ariaei; Adsorptions of Diatomic Gaseous Molecules (H_2, N_2 and CO) on the Surface of $Li^+@C_{16}B_8P_8$ Fullerene–Like Nanostructure: Computational Studies. Adv. J. Chem. B 1 (2019) 29–36 doi: 10.33945/SAMI/AJCB.2019.1.6